A&A 398, 639–646 (2003)
DOI: 10.1051/0004-6361:20021570

Astronomy & Astrophysics

X-ray and gamma-ray emission from millisecond pulsars

L. Zhang[1] and K. S. Cheng[2]

[1] Department of Physics, Yunnan University, Kunming, Yunnan, PR China
[2] Department of Physics, University of Hong Kong, Pokfulam Road, Hong Kong, PR China

Received 23 July 2002 / Accepted 17 October 2002

Abstract. We present a self-consistent model to describe X-ray and γ-ray emission from millisecond pulsars (MSPs). The X-rays of MSPs are produced by the backflow of primary charged particles from the outer gap and most likely consist of three components, two thermal components and one power law component if there is a strong multipole magnetic field on the stellar surface. The backflow of ultra-relativistic particles emits photons with energies about several tens of GeV via curvature radiation. These photons cause an electromagnetic cascade about 2–3 stellar radii above the polar cap. The synchrotron radiation of these cascade $e^{\pm}$ pairs produces hard X-rays with a power law index $\sim$1.5. Near 10^5 cm above the stellar surface, the primary charged particles encounter the strong surface magnetic field, which alters the local radius of curvature greatly, and they quickly loose more than half of their remaining energies to curvature radiation. These curvature photons heat up the polar cap area with a radius $\sim 10^5$ cm, which produce the softer thermal X-ray component. Finally, the primary charged particles deposit their remaining energies in a much smaller polar cap area, which corresponds to the footprints of outer gap and produce the medium hard X-ray component. γ-rays are produced in the outer gap through synchro-curvature radiation. We have applied this model to the MSPs which emit pulsed X-rays and likely γ-rays such as PSR J0437-4715, PSR J2124-3358, PSR J0218+4232 and PSR B1821-24. Our results give an agreement between predicted spectrum and the observed spectrum of MSP emission.

Key words. gamma rays: theory – stars: pulsars: general

1. Introduction

Becker & Trümper (1999) have reported 9 millisecond pulsars which are detected to emit X-ray emission in the ROSAT energy range. Four of them have been firmly detected to emit pulsed X-rays. They are PSR J0437-4715 (Becker & Trümper 1993; Halpern et al. 1996), PSR B1821-24 (Saito et al. 1997), PSR J2124-3358 (Becker & Trümper 1997) and PSR J0218+4232 (Verbunt et al. 1996; Kuiper et al. 1998). Two natural sources of thermal X-rays are neutron star cooling and polar cap heating. According to standard cooling models (a general review cf. Tsuruta 1998), MSPs are too cold to emit strong thermal X-rays because they are old neutron stars re-activated by accretion (Alpar et al. 1982). Even internal heating mechanisms are included, like frictional heating of superfluid (Shibazaki & Lamb 1989) and crust cracking (Cheng et al. 1992; Chong & Cheng 1993), the surface temperature of MSPs is unlikely to exceed a few times 10^5 K. In polar cap heating models (e.g. Cheng & Ruderman 1980; Arons 1981; Beskin et al. 1993; Zhang & Harding 2000), models predict that the polar cap temperature should be 10^6 K to 10^7 K in a polar cap radius $R_{\rm pc} = (R^3\Omega/c)^{1/2}$. Recently, Zavlin et al. (2002) report the spectral and timing observations of the nearest MSP J0437-4715. They find that the X-ray spectrum of this pulsar consist of three components, one power law and two thermal. The harder thermal component has a temperature $\sim 2 \times 10^6$ K, which is consistent with some polar cap heating models but the radius of this component is only $\sim 10^4$ cm, which is one order of magnitude smaller than polar cap radius. Furthermore the thermal X-ray pulses appear to coincide in time with the pulse of the non-thermal component, which is hard to reconcile in terms of polar cap models.

Moreover, Verbunt et al. (1996) (also see Kuiper et al. 1999) noticed that PSR J0218+4232 is positionally consistent with the EGRET high energy source 2EG J0220+4228 (Thompson et al. 1995), detected above 100 MeV at a $>5\sigma$ significance. Fierro (1995) obtained the γ-ray flux (>100 MeV) of PSR B1821-24 although the spatial coincidence is marginal. All of these motivate us to propose a model to explain the X-ray and γ-ray emission from MSPs.

Wei et al. (1996) have considered γ-ray emission from MSPs in the context of the original outer gap model (Cheng et al. 1986a, 1986b). In their model, the pulsed γ-rays with $E_\gamma \leq E_{\rm crit}$ are produced inside the light cylinder, where $E_{\rm crit}$ is the threshold energy in which electrons/positrons cascade will occur. Moreover, the unpulsed γ-rays are produced outside the light cylinder. Therefore the γ-rays from the MSPs consist of pulsed and unpulsed components. Zhang & Cheng (1997) have proposed a pulsar model to describe the X-ray and γ-ray emission from normal pulsars. Furthermore,

Send offprint requests to: L. Zhang,
e-mail: astroynu@public.km.yn.cn

Cheng et al. (1998) have applied the model to explain X-ray emission from pulsars. Cheng & Zhang (1999) have further modelled multi-component X-ray emission from the pulsars. Bulik et al. (2000) have used the polar-cap model calculations of Rudak & Dyks (1998) to predict the general properties of spectral features of high-energy emission above 1 MeV from millisecond pulsars. X-ray emission from polar-cap models is expected from the backflow current. However, Arons & Scharlemann (1979) estimated that only 10% of charged particles produced in polar gap can stream back to the neutron star because the electric field in polar gap boundary is not strong enough to return all oppositely charged particles. However, actually how many $e^{\pm}$ accelerated in the polar cap can stream back to the neutron star are not known and why two-component X-ray can be produced is not clear. So we will not consider the thermal X-ray due to the charged particles accelerated in the polar gap.

In this paper, we consider a model that describes both the X-ray and γ-ray emission from MSPs. The main difference between this model and the model given by Zhang & Cheng (1997) is that the possible effect of a multipole magnetic field near the MSP surface is taken into account in this model. In the model of Zhang & Cheng (1997), the X-rays produced by the return particles cannot be reflected through resonant cyclotron scattering because of weak dipole magnetic field for MSPs, so only one thermal and one power-law component of X-ray spectrum are predicted. In the present model, one power-law and two thermal components of X-ray spectrum are predicted because of the local strong magnetic field. Furthermore, the outer gap size, which determines the properties of γ-rays, is also affected. In Zhang & Cheng (1997), the resonant cyclotron scattering can reflect the hard X-rays back to stellar surface, which are re-emitted as soft X-rays, and the outer gap size is determined by the collisions between γ-rays and soft X-rays. In MSPs, which do not have resonant cyclotron scattering, the gap size is directly determined by the collisions between hard X-rays and γ-rays. In Sect. 2, the model is presented. Applications of this model to PSR J0437-4715, PSR J2124-3358, PSR J0218+4232 and PSR B1821-24 are given in Sect. 3. A brief discussion is made in Sect. 4.

2. A model of X-ray and gamma-ray production

2.1. Pure dipole magnetic field near the stellar surface

According to Zhang & Cheng (1997), for a self-sustained outer gap of pulsar, $e^{\pm}$ pairs needed to control the size of the outer gap are produced by photon-photon pair production resulting from the collisions between the curvature photons in the outer gap and the thermal X-rays from the neutron star surface. The average energy of the curvature photons is related to the fractional size of the outer gap (f) by $E_\gamma \approx 2\times10^8 f^{3/2} B_{12}^{3/4} P^{-7/4}$ eV, where P is the pulsar period in units of seconds, B_{12} is the dipolar magnetic field in units of 10^{12} G and the radius of the neutron star (R) is assumed to be 10^6 cm. These thermal X-rays are produced by collision of the backflowing current with the neutron star surface since half of the primary $e^{\pm}$ pairs in the outer gap will move toward the star and lose their energy via the curvature radiation. The return particle flux can be approximated by $\dot{N}_{e^{\pm}} \approx \frac{1}{2} f \dot{N}_{GJ}$, where $\dot{N}_{GJ}$ is the Goldreich-Julian particle flux (Goldreich & Julian 1969). Although most of the energy of the primary particles will be lost on the way to the star via curvature radiation, about $10.6P^{1/3}$ ergs per particle will still remain and finally deposit on the stellar surface. This energy will be emitted in the form of X-rays from the stellar surface (Halpern & Ruderman 1993). The characteristic energy of X-rays is given by $E_X^h \approx 3kT \approx 1.2\times10^3 P^{-1/6} B_{12}^{1/4}$ eV. The keV X-rays from a hot polar cap will be reflected back to the stellar surface due to the cyclotron resonance scattering assuming that there is large density of magnetic produced $e^{\pm}$ pairs near the neutron star surface (Halpern & Ruderman 1993), and eventually re-emit soft thermal X-rays with characteristic energy $E_X^s \approx 0.1 f^{1/4} P^{-1/4} E_X^h$.

Despite the fact that X-ray photon density is very low, every pair produced by means of X-ray and curvature photons collision can emit 10^5 photons in the outer gap. Such huge multiplicity can produce sufficient number of $e^{\pm}$ pairs to sustain the gap as long as the center of mass energy of X-ray and curvature photon is higher than the threshold energy of the electron/positron pair production, i.e. $E_X E_\gamma(f) \geq (m_e c^2)^2$. From the condition for the photon-photon pair production, the size of the outer gap limited by the soft thermal X-rays from the neutron star surface can be determined as

$$f_s = 5.5 \cdot P^{26/21} B_{12}^{-4/7}. \quad (1)$$

This however is valid for the canonical pulsars. It may not hold true for MSPs where the surface magnetic fields are too weak to produce magnetic pairs. Therefore the electron screening, which is responsible for the cyclotron resonant scattering, might not exist. Even in the case where there might exist a strong local magnetic field near the stellar surface (Cheng et al. 1998; Cheng & Zhang 1999), these pairs are produced locally and hence unlikely reflect most of hard X-rays back to the entire stellar surface.

2.2. Strong multipole magnetic field near the stellar surface

It has been proposed that there is strong multipole magnetic field near the stellar surface although a global dipole magnetic field gives a good description of the magnetic field far from the star (Ruderman & Sutherland 1975; Blandford et al. 1983; Romani 1990; Ruderman 1991a–c; Arons 1993). Ruderman & Sutherland (1975) assumed that there should be a strong multipole surface magnetic field with a radius of curvature $\sim10^6$ cm in order to explain the copious γ – B pair production process. Theoretically, it has been argued that the neutron star magnetic field is produced by currents flowing in a thin crustal layer of thickness $\Delta r \ll R$, where $R = 10^6$ cm is the neutron star radius (e.g. Blandford et al. 1983; Romani 1990). Thus, the actual surface magnetic field should be dominated by the multipoles. Arons (1993) suggested that the surface magnetic field should be a superposition of clumps with a typical size Δr covering the whole surface of a neutron star. The surface magnetic field can be approximated by $B_s \sim B_d^0 (R/\Delta r)^n$, where B_d^0 is the global

surface dipole component which can be inferred from the pulsar spin down rate, $n = 1$ and 2 represent coherent and incoherent superpositions of dipole moments of clumps respectively. Since Δr must be less than the thickness of the crust ($\sim 10^5$ cm), B_s should be easily 10–10^3 of B_d^0.

Here we assume that there is a strong local magnetic field located in a region near the polar cap for the millisecond pulsar with outer gaps. The typical radius of curvature l of this local magnetic field is of the order of the crust thickness of the star (i.e. $l \sim 10^5$ cm), which is much less than the dipolar radius of curvature s of the dipolar field component near stellar surface. At a certain distance δr above the stellar surface, the local magnetic field is equal to the dipole magnetic field, i.e.

$$B_s^0 \left(\frac{l+\delta r}{l}\right)^{-(m+1)} = B_d^0 \left(\frac{R+\delta r}{R}\right)^{-3}, \quad (2)$$

where B_s^0 and B_d^0 are the local surface and global dipole fields at the stellar surface. From this equation, we can determine $\delta r/l$ for given B_s^0/B_d^0 and m. The local magnetic field is a localized dipole field for $m = 2$, e.g. a sunspot structure (Ruderman 1991a, 1991b, 1991c). From Eq. (2), for the localized dipole field, we have

$$\frac{\delta r}{l} = \frac{(B_s^0/B_d^0)^{1/3} - 1}{1 - (l/R)(B_s^0/B_d^0)^{1/3}}. \quad (3)$$

In the region $R + \delta r$ to R, the local magnetic field will dominate over the global dipolar field. The electrons/positrons leaving the outer gap and moving towards the star emit curvature photons with a characteristic energy

$$E_\gamma(r_{\rm in}) \approx 2.4\times 10^{10} f_m^{3/2} \times P_{-3}^{-7/4} \left(\frac{B_d^0}{10^8 {\rm G}}\right)^{3/4} \left(\frac{r_{\rm in}}{R_L}\right)^{-13/8} {\rm eV}, \quad (4)$$

where R_L is the radius of light cylinder, $r_{\rm in}$ is the inner boundary of the outer gap which is about $(4/9)R_L/\tan^2\alpha$ if the magnetic inclination angle α is not less than 45° (e.g. Halpern & Ruderman 1993) and f_m is the fractional size of the outer gap (different from that given in Eq. (1) due to the insufficient screening) determined by the pair production process. Because of the much smaller radius of curvature, the return particles from the outer gap reaching the distance δr along the magnetic field lines lose their remaining energy (Halpern & Ruderman 1993)

$$E_e(R+\delta r) \approx 1.1 P_{-3}^{1/3} \ {\rm ergs} \quad (5)$$

through curvature radiation, which will become $e^\pm$ pairs by the strong local field, and these energies will deposit on an effective area $A_{\rm eff}^{(1)}$ of the stellar surface. Therefore, the thermal luminosity can be expressed as

$$L_X^{\rm th1} = E_e(R)\dot{N}_{e^\pm} \approx 1.4\times 10^{32} f_m \left(\frac{B_d^0}{10^8 {\rm G}}\right) P_{-3}^{-5/3} \ {\rm ergs\ s^{-1}}. \quad (6)$$

The effective area over which the $e^\pm$ pairs collide with the stellar surface can be estimated as

$$A_{\rm eff}^{(1)} \sim \pi(\delta r)^2, \quad (7)$$

which depends on the ratio of B_s^0 to B_d^0 and m. So the temperature of thermal emission is given by

$$T_m^{(1)} = \left(\frac{L_X}{A_{\rm eff}\sigma_{\rm SB}}\right)^{1/4} \approx 3.0\times 10^6 f_m^{1/4} \left(\frac{B_d^0}{10^8\ {\rm G}}\right)^{1/4} P_{-3}^{-5/12} \delta r_5^{-1/2}\ {\rm K}, \quad (8)$$

where $\delta r_5 = \delta r/10^5$ cm. Moreover, although the return particles lose their energy on the way from the outer gap to the stellar surface along the magnetic field lines, the energy of

$$E_e(R) = m_e c^2 \gamma(R) \approx m_e c^2 \frac{\gamma(R+\delta r)}{(1+(\gamma(R+\delta r)/\gamma_s(R))^3)^{1/3}} \quad (9)$$

will deposit on the area $A_{\rm eff}^{(2)}$ of the stellar surface, which is

$$A_{\rm eff}^{(2)} \sim \frac{B_d^0}{B_s^0} f_m \pi r_p^2, \quad (10)$$

where $\gamma_s(R) \equiv (m_e c^2 l^2/(2e^2\delta r))^{1/3}$ ($\gamma(R) \approx \gamma_s(R)$, $\gamma(R+\delta r) \approx 1.3\times 10^6 P_{-3}^{1/3}$, $l_5 = l/10^5$ cm, and $r_p = R(R/R_L)^{1/2}$ is the radius of the polar cap). If $\gamma^3(R+\delta r) \gg \gamma^3(R)$, Eq. (9) becomes

$$E_e(R) \sim 0.45 l_5^{2/3} \delta r_5^{-1/3} \ {\rm ergs}. \quad (11)$$

We want to point out that for young canonical pulsars ($P \sim 0.1$ s), the energy given in Eqs. (11) or (9) is negligible in comparing with that in Eq. (5). But this energy becomes important for weak field millisecond pulsars because Eqs. (11) and (5) are comparable but the energy shown in Eq. (11) is deposited in a much smaller area which plays a dominant role in hard thermal X-ray emission ($E_x \sim$ KeV). The thermal luminosity is given by

$$L_X^{\rm th2} = E_e(R)\dot{N}_{e^\pm} \approx \frac{L_X^{\rm th1}}{(1+(\gamma(R+\delta r)/\gamma_s(R))^3)^{1/3}} \quad (12)$$

and the corresponding temperature is

$$T_m^{(2)} \approx 7.8\times 10^6 f_m^{1/4} \left(\frac{B_s^0}{10^{11}\ {\rm G}}\right)^{1/4} P_{-3}^{-1/6} \left(1+\left(\frac{\gamma(R+\delta r)}{\gamma_s(R)}\right)^3\right)^{-1/12} {\rm K}. \quad (13)$$

From Eqs. (8) and (13), $T_m^{(2)}/T_m^{(1)} \sim 0.4\ (B_s^0/B_d^0)^{1/4} P_{-3}^{1/6} l_5^{1/6} \delta r_5^{5/12}$, so we have $T_m^{(2)} > T_m^{(1)}$ if $(B_s^0/B_d^0) > 100$ for the millisecond pulsars. The fractional size of the outer gap can be determined by the collision between the curvature photons in the outer gap and the thermal X-rays with a temperature $T_m^{(1)}$ from the neutron star surface through photon-photon pair production process, which is

$$f_m \approx 7.0\times 10^{-2} P_{-3}^{26/21} \left(\frac{B_d^0}{10^8\ {\rm G}}\right)^{-4/7} \delta r_5^{2/7}. \quad (14)$$

We would like to point out that the effect of inclination angle (α) on the fractional size of the outer gap is neglected. This factor can reduce the fractional size of the outer gap by a factor

Table 1. Observed and expected quantities for 9 millisecond pulsars. Columns 1 to 5 list pulsar name, period, surface magnetic field, distance and observed X-ray luminosity respectively. Column 6 lists the fractional size of the outer gap for each pulsar, which is estimated using Eq. (14). Columns 7 and 8 are the temperatures which are estimated using Eqs. (8) and (13) respectively. Column 9 is the predicted X-ray luminosity (one power-law and two thermal components) for each pulsar. In our estimate, the parameters used are $l = 10^5$ cm, $m = 2$ and $B_{\rm s}^0/B_{\rm d}^0 = 100$.

Pulsar	P ms	$\log B$ Gauss	d kpc	$\log L_{\rm X}^{\rm obs}$ erg/s	$f_{\rm m}$	$T_{\rm m}^{(1)}$ 10^6 K	$T_{\rm m}^{(2)}$ 10^6 K	$\log L_{\rm X}^{\rm theo}$ erg/s
B1957+20	1.60	8.14	1.53	31.93	0.180	0.67	1.46	32.10
J0751+1807	3.47	8.23	2.02	31.60	0.419	0.62	2.54	31.26
J1012+5307	5.25	8.45	0.52	30.20	0.523	0.64	3.01	31.25
J1024-0719	5.16	8.49	0.35	29.30	0.484	0.64	3.03	31.27
J1744-1134	4.07	8.27	0.26	29.48	0.482	0.62	2.69	31.22
J0437-4715	5.75	8.54	0.18	30.98	0.519	0.65	3.15	31.27
B1821-24	3.05	9.35	5.50	33.20	0.083	0.84	3.22	32.56
J0218+4232	2.32	8.63	5.70	32.75	0.148	0.73	2.36	32.10
J2124-3358	4.93	8.36	0.25	30.18	0.543	0.63	2.90	31.22

of several if the inclination is larger than 50° (Zhang & Cheng 2002). It is because the null surface can move in, close to the star for a large inclination angle, and consequently the average size of the outer gap is significantly decreased. Furthermore, a small size of outer gap can also change the radiation and pair production processes in the outermagnetosphere. For typical MSP parameters, it could change from Vela-like/Geminga-like mechanisms for $\alpha \ll 50°$ to Crab-like mechanisms (Cheng et al. 1986a, 1986b; Zhang & Cheng 1997).

As suggested by Zhang & Cheng (1997), most of the energy of the return particles obtained from the outer gap will not be deposited on the polar area, instead, many curvature photons will be produced around δr above the surface if $B_{\rm s} \gg B_{\rm d}$, and then many $e^{\pm}$ pairs will be created by the magnetic pair production process in the strong local magnetic field if the condition of magnetic pair production is satisfied. Because the local magnetic field is strong, it dominates the region from $R + \delta r$ to the star. However, the magnetic moment of the strong local magnetic field is not larger than that of the dipole field, which means

$$B_{\rm s}^0 \leq 10^{11} \left(B_{\rm d}^0/10^8\ {\rm G}\right) l_5^{-3}\ {\rm G}. \tag{15}$$

for $m = 2$, which can be also derived from Eq. (3). Moreover, the position where secondary $e^{\pm}$ pairs are produced through the magnetic pair production can be estimated by using $(E_\gamma/2m_{\rm e}c^2)(B_{\rm s}/B_{\rm q}) \geq 1/15$, where $B_{\rm q} = 4.4 \times 10^{13}$ G. Assuming that the secondary $e^{\pm}$ pairs are produced at the position $\delta r_{\rm s}$ above the stellar surface, we have

$$\frac{\delta r_{\rm s}}{R} \approx \frac{l}{R}\left[\left(\frac{15B_{\rm s}^0}{B_{\rm q}}\frac{E_\gamma}{2mc^2}\right)^{1/3} - 1\right], \tag{16}$$

which means that the secondary $e^{\pm}$ pairs can be produced near the stellar surface if $(15B_{\rm s}^0/B_{\rm q})(E_\gamma/2mc^2) > 1$. Therefore, non-thermal X-rays will be produced by the synchrotron radiation of secondary $e^{\pm}$ pairs created in the strong pulsar magnetic field near the neutron star surface by curvature photons emitted by charged particles on their way from the outer gap to the neutron star surface. The luminosity of non-thermal X-rays from MSPs can be expressed as

$$L_{\rm X}^{\rm non} \sim 2 \times 10^{-4} f_{\rm m}^{-1/2} P_{-3}^{-0.25} \left(\frac{B_{\rm d}^0}{10^8{\rm G}}\right)^{-0.75} \left(\frac{r_{\rm s}}{R}\right)^2 \left(\frac{r_{\rm in}}{R_{\rm L}}\right)_{\rm min}^{-19/8} L_{\rm sd}, \tag{17}$$

where $L_{\rm sd} \approx 3.8 \times 10^{35} (P/{\rm ms})^{-4} (B/10^8\ {\rm G})^2$ ergs s^{-1} is the spin-down power. It should be pointed out that the condition $r_{\rm s}/R \geq 1$ must be satisfied if $e^{\pm}$ pairs are produced in the region from $(R + \delta r)$ to the star. Otherwise, there is the non-thermal X-ray component. Therefore, the X-ray spectrum from a millisecond pulsar can be expressed as a combination of two thermal components with typical temperature $T_{\rm m}^{(1)}$ and $T_{\rm m}^{(2)}$ and one non-thermal component with spectral index $\beta \sim 1.5$.

For the γ-ray production, according to Zhang & Cheng (1997), the γ-rays are produced by the synchro-curvature radiation (Cheng & Zhang 1996) in the outer gap which depends sensitively on the local curvature radius. The luminosity of γ-rays can be given

$$L_\gamma \approx 3.8 \times 10^{35} f_{\rm m}^3 P_{-3}^{-4} \left(\frac{B_{\rm d}^0}{10^8\ {\rm G}}\right)^2\ {\rm ergs\ s^{-1}}. \tag{18}$$

As pointed out by Zhang & Cheng (1997), the radiation spectrum produced by the accelerated particles with a power-law distribution in the outer gap depends on two parameters, $x_{\rm min} = (r_{\rm in}/R_{\rm L})^{1/2}$ and $x_{\rm max}$. When the inclination angle α is large, then $x_{\rm min} \sim 2/(3\tan\alpha)$. The quantity $x_{\rm max}$ depends on χ and f. For a very thick outer gap and a nearly aligned rotator, $x_{\rm max} \sim 2$. Furthermore, when the particle energy density is comparable to that of the local magnetic energy density, the local radius of curvature can become larger.

As an example, we assume that $l \sim 10^5$ cm, $B_{\rm s}^0/B_{\rm d}^0 = 100$ and $m = 2$. So we have $\delta r \sim 6.8 \times 10^5$ cm from Eq. (2) and $A_{\rm eff} \sim 1.45 \times 10^{12}$ cm^2. In order to compare with the ROSAT observed data, we have calculated the expected X-ray luminosities in the ROSAT energy range (0.1–2.4 KeV) for 9 millisecond pulsars. In Table 1, we list our model results and the observed data, where $x_{\rm min} = 0.5$ is used. It should be pointed out that the $B_{\rm s}^0/B_{\rm d}^0$, $x_{\rm min}$ and l for different millisecond pulsars should be different although the expected X-ray luminosities are not inconsistent with the observed those. In other

words, we need to use different values of these three parameters in order to compare our results with the observed data.

3. The applications

We use our model to explain the X-ray and γ-ray emission from the millisecond pulsars which emit pulsed X-rays and likely γ-rays such as PSR J0437-4715, PSR J2124-3358, PSR J0218+4232 and PSR B1821-24. According to our model, the X-ray emission from a millisecond pulsar consists of two thermal and one non-thermal X-ray components, and high energy γ- rays are produced in the outer gaps of millisecond pulsar's magnetosphere. In our calculations, we assume that $m = 2$, i.e. the local magnetic field is a dipole field, so the model parameters are B_s^0/B_d^0, l and $x_{\min}$. If the inclination angle of a pulsar is known, then the $x_{\min}$ can be determined, otherwise, $x_{\min}$ is adjusted to make the expected X-ray energy flux be the same as the observed for given B_s^0/B_d^0 and l.

3.1. PSR J0437-4715

PSR J0437-4715, which was discovered by Johnston et al. (1993), is a millisecond pulsar with a period 5.75 ms and a period derivative $(0.8 \pm 0.7) \times 10^{-20}$ s s^{-1} which is in a close 5.74 day circular orbit around a $\sim$0.25 $M_\odot$ white dwarf companion (e.g. Becker & Trümper 1999). Its surface dipole magnetic field is $\sim 3.2 \times 10^8$ G if a global dipole magnetic field in the magnetosphere is assumed, and its distance is (178±26) pc. The inclination angle of the pulsar is 35° (Manchester & Johnston 1995). The X-ray emission from this pulsar has been observed by ROSAT and ASCA and the spectrum has been obtained (Becker & Trümper 1993, 1997, 1999; Kawai et al. 1998). The observed luminosity of this pulsar is listed in Table 1. Halpern et al. (1996) considered the soft X-ray properties of this pulsar using EUVE and ROSAT data. The observed X-ray spectrum can be fitted by a double blackbody model, i.e. the thermal X-rays with typical temperature $T_1 = (4 - 12) \times 10^5$ K are produced on a larger area (A_1) less than 200 km^2 and the thermal X-rays with $T_2 = (1.0\text{–}3.3) \times 10^6$ K are from a smaller area (A_2) with radius 50–600 m (Halpern et al. 1996). More recently, Becker & Trümper (1999) pointed out that the temperatures of the double black body components are 1.2×10^6 K derived from ROSAT data and $\sim (3.0 \pm 0.5) \times 10^6$ K derived from ASCA data respectively and the X-ray energy flux is $(1.9 \pm 0.2) \times 10^{-12}$ ergs cm^{-2} s^{-1} in 0.1–2.4 KeV. For the γ-ray emission from this pulsar, the upper limit of observed flux above 100 MeV is 1.51×10^{-7} cm^{-2} s^{-1} (Fierro et al. 1995).

In our calculations, we use the observed inclination angle of this pulsar to estimate $x_{\min}$, which is $x_{\min} \sim 0.95$, then we choose the B_s^0/B_d^0 and l to fit the observed X-ray energy flux and we have $B_s^0/B_d^0 \approx 800$ and $l_5 \approx 0.15$. Furthermore, we have $T_m^{(1)} \sim 1.19 \times 10^6$ K, $T_m^{(2)} \sim 2.71 \times 10^6$ K and $f_m \sim 0.43$. The ratio of areas corresponding to temperature $T_m^{(1)}$ and $T_m^{(2)}$ is $A_{\rm eff}^{(1)}/A_{\rm eff}^{(2)} \sim 455$, which is consistent with the observed results ranging from 10^{-4}–10^{-2} given by Halpern et al. (1996). Moreover, the non-thermal X-ray flux expected by our model for PSR J0437-4715 is less than the thermal X-ray one because of large value of $x_{\min}$. In our calculation of X-ray spectrum,

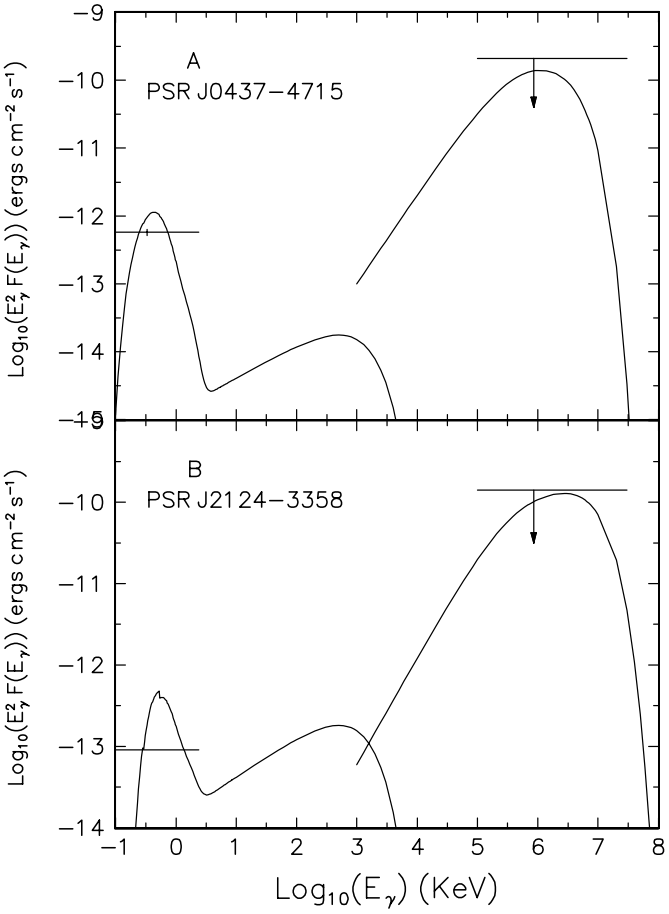

Fig. 1. Comparison of our model results (solid curves) with the observed data for the spectra of X-rays and γ-rays from PSR J0437-4715 and PSR J2124-3358. **A)** The observed pulsed X-ray energy flux of PSR J0437-4715 is taken from Becker & Trümper (1999) and the upper limit of γ-rays in the energy range from 100 MeV to 30 GeV is taken from Fierro et al. (1995). **B)** The observed pulsed X-ray energy flux of PSR J2124-3358 is taken from Becker & Trümper (1997) and the upper limit of γ-rays in the energy range from 100 MeV to 30 GeV is obtained by assuming that EGRET threshold for point source detection above 100 MeV is no lower than 10^{-7} cm^{-2} s^{-1} (Fierro 1995).

$N_H = 8.5 \times 10^{19}$ cm^{-2} (Becker & Trümper 1999), and the photoelectric cross section of the interstellar medium (Morrison & McCammon 1983) are used. Furthermore, we assume that $x_{\max} \sim 2$ and then calculate the γ-ray spectrum based on the model proposed by Zhang & Cheng (1997). In panel A of Fig. 1, the comparison of observed and expected spectrum from X-ray band to γ-ray band is shown, where the observed pulsed X-ray energy flux is used.

After completion of this manuscript, we find that Zavlin et al. (2002) have reported new X-ray results of PSR J0437-4715 observed by Chandra. They find that the X-ray spectra of PSR J0437-4715 can be described two thermal components plus one power law component with a spectral index ≈2.2. The temperatures and the radii of those two thermal components are 2.1 MK and 0.12 km, and 0.54 MK and 2.0 km respectively. These parameters are consistent with our parameters used here.

3.2. PSR J2124-3358

PSR J2124-3358 is an isolated millisecond pulsar with a period 4.93 ms and a period derivative 1.08×10^{-20} s s^{-1}. It was discovered by Bailes et al. (1997) and its distance is $d \sim 250$ pc. X-rays from this pulsar have been detected by ROSAT (Becker & Trümper 1997). Total and pulsed X-ray luminosities are $\sim 2.24 \times 10^{30}$ $(d/250$ kpc$)^2$ ergs s^{-1} and $\sim 6.9 \times 10^{29}$ $(d/250$ kpc$)^2$ ergs s^{-1} respectively. No information on the pulsar γ-ray emission in EGRET energy range is available. However, ASCA has observed this pulsar on 1998 May 9 and the X-ray spectrum in 0.6-10 KeV band was obtained (Sakurai et al. 2001). The X-ray spectrum can be fitted with a single blackbody model with a temperature $kT = 0.31$ (+0.08, −0.06) KeV.

The period and global dipole magnetic field of PSR J2124-3358 are similar to those of PSR J0437-4715, so the expected X-ray luminosity in ROSAT energy range seems to be dominated by thermal X-ray components. $l_5 = 0.3$ and $B^0_{\rm d}/B^0_{\rm s} = 10^{-2}$ are chosen to fit the observed X-ray luminosity, so we have $T^{(1)}_{\rm m} \sim 1.28 \times 10^6$ K, $T^{(2)}_{\rm m} \sim 3.03 \times 10^6$ K and $f_{\rm m} \sim 0.34$. These parameters are consistent with the spectrum obtained by ASCA (Sakurai et al. 2001). We find that the non-thermal X-ray flux for thus parameters is much less than the thermal ones if $x_{\rm min} > 0.6$, so we use $x_{\rm min} = 0.7$ to calculate the γ-ray spectrum of this pulsar. In our calculation, $N_{\rm H} = 5.0 \times 10^{20}$ cm^{-2} (Becker & Trümper 1997) is used. In panel B of Fig. 1, the comparison of observed and expected spectrum from X-ray band to γ-ray band is shown.

3.3. PSR J0218+4232

PSR J0218+4232 is a millisecond pulsar with a period 2.32 ms and a period derivative 8.0×10^{-20} s s^{-1} which is in a 2 day binary orbit with a ~ 0.2 $M_\odot$ white dwarf companion (Navarro et al. 1995). From the dispersion measure, the distance is about 5.7 kpc. X-rays from this pulsar have been detected by ROSAT (Verbunt et al. 1996; Kuiper et al. 1998; Becker & Trümper 1999). Total and pulsed energy fluxes are 1.5×10^{-13} ergs cm^{-2} s^{-1} and $(3.9 \pm 1.4) \times 10^{-14}$ ergs cm^{-2} s^{-1} respectively (Kuiper et al. 1998). The γ-rays have also been detected by EGRET (Verbunt et al. 1996; Kuiper et al. 1999; Kuiper et al. 2000). The pulse shape and energy spectrum of this pulsar in the energy band 1–10 keV observed with BeppoSAX was presented (Mineo et al. 2000). The pulse profile is characterized by two peaks separated by 169° and the pulsed spectrum is best described by a power-law of photon index 0.61. The X-ray luminosity in 2–10 keV is $1.3 \times 10^{32}\theta$ erg/s, where θ is the solid angle spanned by the emission beam.

We choose following parameters: $l_5 = 1.0$ and $B^0_{\rm d}/B^0_{\rm s} = 10^{-2}$ in our calculations, then we have $\delta r \sim 6.8 \times 10^5$ cm and $f_{\rm m} \sim 0.15$. Furthermore, compared to the observed luminosity of pulsed X-rays from PSR J0218+4232 which is $\sim 10^{32}$ ergs s^{-1}, we have $x_{\rm min} \approx 0.46$. Therefore, the efficiency of converting spin-down power into γ-rays is about 0.34%. According to Verbunt et al. (1996), the time-averaged flux of γ-ray (>100 MeV) from 2EG J0220+4228 is about 1.7×10^{-8} photons cm^{-2} s^{-1}. The corresponding luminosity is about 8×10^{33} ergs s^{-1}, where the solid angle $\Delta\Omega$ has been assumed to be 1 sr. The observed efficiency which spin-down power is converted to γ-rays is about 3%. However, Kuiper et al. (2000) reported circumstantial evidence for the pulsed high-energy gamma-ray from this pulsar, which gave the pulsed γ-ray luminosity $\sim 1.64 \times 10^{34}$ erg/s and it is about 7% of the total spin-down luminosity. According to our model, the spectrum from X-ray to γ-ray for a pulsar can be determined if the pulsar's parameters: period P, magnetic field B, inclination angle α and $x_{\rm max}$ are known. The expected spectrum of X-ray and γ-ray emission from PSR J0218+4232 is shown in the panel A of Fig. 2. In our calculation of X-ray spectrum, $N_{\rm H} = 5 \times 10^{20}$ cm^{-2} and $\beta = -1.5$ (Kuiper et al. 1998), and the photoelectric cross section of the interstellar medium (Morrison & McCammon 1983) are used. For the calculation of the γ-ray spectrum, $x_{\rm min} = 0.46$ (corresponding value of the magnetic inclination angle is about 55°) which is determined by equating the expected X-ray luminosity to the observed one, $x_{\rm max} = 2.0$ and $\Delta\Omega = 1$ sr are used. From Fig. 2A, the expected

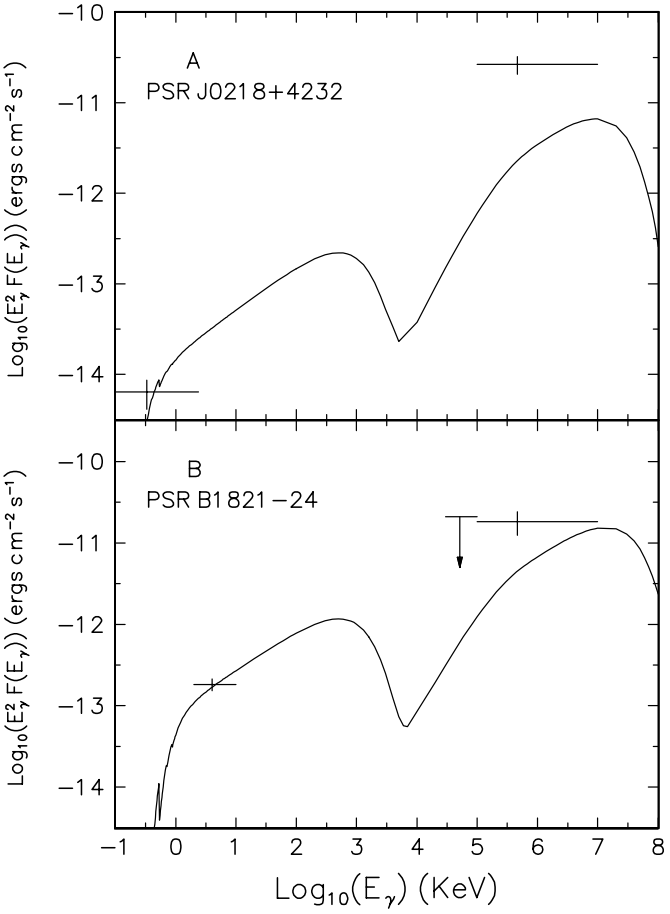

Fig. 2. Comparison of our model results (solid curves) with the observed data for the spectra of X-rays and γ-rays from PSR J0218-4232 and PSR B1821-24. **A)** The observed pulsed X-ray energy flux of PSR J0218-4232 is taken from Becker & Trümper (1999) and the observed γ-ray flux in the energy range from 100 MeV to 10 GeV is taken from Verbunt et al. (1996). **B)** The observed pulsed X-ray energy flux of PSR B1821-24 is taken from Saito et al. (1997) and the observed γ-ray fluxes in the energy ranges from 30 MeV to 100 MeV and from 100 MeV to 10 GeV are taken from Fierro (1995).

γ-ray spectrum is below the observed data given by Verbunt et al. (1996). If the expected γ-ray spectrum is consistent with the observed data, then the solid angle should be ~0.1 sr, which seems too small.

3.4. PSR B1821-24

PSR B1821-24 is an isolated millisecond pulsar in the globular cluster M28. Its period and period derivative are 3.05 ms and 1.62×10^{-18} s s^{-1} respectively, and the distance is about 5.1 kpc. The X-rays have been detected by ROSAT and ASCA (e.g. Danner et al. 1994, 1997; Saito et al. 1997) and γ-ray flux has been observed by EGRET (Fierro 1995).

We apply our model to this millisecond pulsar. The pulsed X-ray component has been observed by ASCA and the pulsed X-ray luminosity is $\sim 9.4 \times 10^{32}$ ergs s^{-1} (Saito et al. 1997). Moreover, the γ-ray emission has been observed by EGRET and γ-ray fluxes are $\leq 4.81 \times 10^{-7}$ cm^{-2} s^{-1} in the energy range from 30 MeV to 100 MeV and $(11.4 \pm 3.6) \times 10^{-8}$ cm^{-2} s^{-1} in the energy range with energy greater than 100 MeV (Fierro 1995). Corresponding observed γ-ray efficiency with energy greater than 100 MeV is ~0.2% if the solid angle is 1 sr. Using the same parameters as those of PSR J0218+4232 except $x_{\rm min} = 0.39$, we have $f_{\rm m} \sim 0.08$. So we obtain that the expected γ-ray efficiency is ~0.06%. In panel B of Fig. 2, the expected spectrum of X-ray and γ-ray emission from PSR B1821-24 is shown, where $N_{\rm H} = 2.8 \times 10^{21}$ cm^{-2}, $\beta = -1.5$ and $\Delta\Omega = 1$ sr are used. It can be seen that the expected spectrum is not inconsistent with the observed data.

4. Discussion

We have presented a model to describe the X-ray and γ-ray emission from MSPs. Assuming that there is a strong multipole magnetic field near the stellar surface (this local magnetic field is estimated by Eq. (2)), the X-rays are produced by the backflow current of the outer gap. These X-rays consist of one power-law and two thermal components: (i) the non-thermal X-rays are produced by the synchrotron radiation of $e^{\pm}$ pairs created in the strong magnetic field near the stellar surface by curvature photons emitted by charged particles on their way from the outer gap to the neutron star surface; (ii) the soft thermal X-rays are produced by heating of polar cap area with a radius 10^5 cm due to the curvature photons of the return particles from the outer gap in the strong local magnetic field; and (iii) the medium hard thermal X-rays result from the polar cap heating by the return particles from the outer gap. The light curves of these two thermal components can have $360^\circ \delta r/(2\pi R) \sim 10^\circ$ phase shift. The phase shift between soft X-rays and synchrotron X-rays could be up to 180°. The X-rays collide with high-energy photons inside the outer gap to sustain the outer gap. The γ- rays are produced in the outer gap. In this model, the condition of the outer gap existence is $f_{\rm m} \leq 1$ (see Eq. (14)), which depends on the typical radius of curvature l, parameters m and $B_{\rm s}^0/B_{\rm d}^0$ (see Eq. (2)). The basic parameters for a given MSP in our model are l, m, $B_{\rm s}^0/B_{\rm d}^0$ and the inclination angle. In Table 1, we have shown that the outer gaps for the known MSPs which are detected to emit X-rays can exist for the parameters $l = 10^5$ cm, $m = 2$, $B_{\rm s}^0/B_{\rm d}^0 = 100$ and $x_{\rm min} \approx 2/3 \tan\alpha = 0.5$. It should be pointed out, however, that the values of local strong magnetic field near the stellar surface, the curvature radius and the magnetic inclination angle are different for various MSPs. Our model predicts that a γ-ray MSP would be a X-ray MSP, or a X-ray MSP which the X-ray emission comes from magnetosphere would be a γ-ray pulsar. Furthermore we have applied our model to the MSPs which emit pulsed X-rays and likely γ-rays such as PSR J0437-4715, PSR J2124-3358, PSR J0218+4232 and PSR B1821-24 (Figs. 1 and 2). Our model results are consistent with the observed data.

Although we suggest that all of these X-ray components are produced by the backflow current of outer gap, it is possible that those two thermal components may result from the following polar cap model. For example, assuming a strong surface field again exist, then the polar cap and the polar cap accelerator has an area described by Eq. (7). In this case the backflow of primary charged particles produced inside the polar cap can easily radiate the harder thermal component. Clearly, part of this thermal energy must be transported along the magnetic field into the stellar interior. Since the multipole should penetrate about 10^5 cm in the crust, subsequently it must spread over an area with radius $\sim 10^5$ cm, which produce softer X-rays with larger emission. However, this scenario may still have difficulty in explaining why the pulses of thermal and non-thermal components are in phase (Zavlin et al. 2002).

Sturner & Dermer (1994) have extended four γ-ray models to the millisecond regime and discussed their predictions for the detectability for known millisecond pulsars. These models are (i) relativistic pulsar wind model (model UN) (e.g. Tavani 1991); (ii) polar cap model-magnetic Compton-induced cascade (model SD) (Dermer & Sturner 1994); (iii) polar cap model-curvature radiation-induced cascade (model HTE) (e.g. Harding et al. 1978; Harding 1981; Daugherty & Harding 1982) and (iv) original outer gap model (model CHR) (Cheng et al. 1986a, 1986b). They found that models UN and SD do not predict any millisecond pulsars which emit γ-rays detected by EGRET, but HTE and CHR predict almost half of the millisecond pulsar sample would be detectable. According to our model, an MSP sample would emit high energy γ-rays if the fractional size of its outer gap is less than unity. However, the energy range of the γ-rays depends on $x_{\rm min}$ which is determined by the observed pulsed X-ray flux.

According to Wei et al. (1996), the γ-rays from MSPs consist of pulsed γ-rays with energy less than ~1 GeV produced inside the light cylinder and unpulsed γ-rays with energy greater than ~1 GeV produced outside the light cylinder. However, our model predicts that the production of the pulsed high energy γ-rays depends on the value of $x_{\rm min}$, and then on the observed X-ray flux. If the observed X-rays are dominated by the non-thermal X-ray component, then the γ-rays can extend to higher energy, say 20–30 GeV (see Fig. 2). Otherwise, only ~GeV γ-ray can be produced.

Acknowledgements. We would like to thank the anonymous referee, whose useful comments helped to improve the manuscript. This work is partially supported by a RGC grant of Hong Kong Government,

the National Natural Scientific Foundation of China (10073008) and the National 973 Projection of China (NKBRSFG 19990754). KSC thanks the hospitality of Tsing Hua University, where part of this work is done.

References

Alpar, M. A., Cheng, A. F., Ruderman, M. A., & Shaham, J. 1982, Nature, 300, 728
Arons, J. 1981, ApJ, 284, 1099
Arons, J. 1993, ApJ, 408, 160
Arons, J., & Scharlemann, E. T. 1979, ApJ, 231, 854
Bailes, M., Johston, S., Bell, J. F., et al. 1997, ApJ, 481, 386
Becker, W., & Trümper, J. 1993, Nature, 365, 528
Becker, W., & Trümper, J. 1997, A&A, 326, 682
Becker, W., & Trümper, J. 1999, A&A, 341, 803
Beskin, V. S., Gurevich, A. F., & Istomin, Ya, N. 1993, Physics of Pulsar Magnetosphere (Cambridge: Cambridge University Press)
Blandford, R. D., Applegate, J. H., & Hernquist, L. 1983, MNRAS, 204, 1025
Bulik, T., Rudak, B., & Dyks, J. 2000, MNRAS, 317, 97
Cheng, A. F., & Ruderman, M. A. 1980, ApJ, 235, 576
Cheng, K. S., Chau, W. Y., Zhang, J. L., & Chau, H. F. 1992, ApJ, 396, 135
Cheng, K. S., Ho, C., & Ruderman, M. A. 1986a, ApJ, 300, 500 (CHR I)
Cheng, K. S., Ho, C., & Ruderman, M. A. 1986b, ApJ, 300, 522 (CHR II)
Cheng, K. S., Gil, J., & Zhang, L. 1998, ApJ, 493, L35
Cheng, K. S., & Zhang, J. L. 1996, ApJ, 463, 271
Cheng, K. S., & Zhang, L. 1999, ApJ, 515, 337
Chong, N., & Cheng, K. S. 1993, ApJ, 417, 279
Danner, R., Kulkarni, S. R., & Thorsett, S. E. 1994, ApJ, 436, L153
Danner, R., Kulkarni, S. R., Saito, Y., & Kawai, N. 1997, Nature, 388, 751
Daugherty, J. K., & Harding, A. K. 1982, ApJ, 252, 337
Dermer, C. D., & Sturner, S. J. 1994, ApJ, 420, L75
Fierro, J. M. 1995, Ph.D. Thesis, Stanford University
Fierro, J. M., Arzoumanian, Z., Bailes, M., et al. 1995, ApJ, 447, 807
Goldreich, P., & Julian, W. H. 1969, ApJ, 157, 869
Johston, S., Lorimer, D. R., Harrison, P. A., et al. 1993, Nature, 361, 613
Halpern, J. P., & Ruderman, M. A. 1993, ApJ, 415, 286
Halpern, J. P., Martin, C., & Marshall, H. L. 1996, ApJ, 462, 908
Harding, A. K. 1981, ApJ, 245, 267
Harding, A. K., Tademaru, E., & Esposito, L. W. 1978, ApJ, 225, 226
Kawai, N., Tamura, K., & Saito, Y. 1998, Adv. Space Res., 21, 213
Kuiper, L., Hermsen, W., Verbunt, F., & Belloni, T. 1998, A&A, 336, 545
Kuiper, L., Hermsen, W., Verbunt, F., Belloni, T., & Lyne, A. 1999, ApL&C, 38, 33
Kuiper, L., Hermsen, W., Verbunt, F., et al. 2000, A&A, 359, 615
Mineo, T., Cusumano, G., Kuiper, L., et al. 2000, A&A, 355, 1053
Morrison, R., & McCammon, D. 1983, ApJ, 270, 119
Navarro, J., de Bruyn, A. G., Frail, D. A., et al. 1995, ApJ, L55
Romani, R. W. 1990, Nature, 347, 741
Rudak, B., & Dyks, J. 1998, MNRAS, 295, 337
Ruderman, M. A., & Sutherland, P. 1975, ApJ, 196, 57
Ruderman, M. A. 1991a, ApJ, 366, 261
Ruderman, M. A. 1991b, ApJ, 382, 576
Ruderman, M. A. 1991a, ApJ, 382, 587
Sakurai, I., Kawai, N., Torii, K., et al. 2001, PASJ, 53, 535
Shibazaki, N., & Lamb, F. 1989, ApJ, 346, 808
Saito, Y., Kawai, N., Kamae, T., et al. 1997, ApJ, 477, L37
Sturner, S. J., & Dermer, C. D. 1994, A&A, 281, L101
Tavani, M. 1991, ApJ, 379, L69
Thompson, D. J., Bertsch, D. L., Dingus, B. L., et al. 1995, ApJS, 101, 259
Tsuruta, S. 1998, Phys. Rep., 292, 1
Verbunt, F., Kuiper, L., Belloni, T., et al. 1996, A&A, 311, L9
Wei, D. M., Cheng, K. S., & Lu, T. 1996, ApJ, 468, 207
Zavlin, V. E., Pavlov, G. G., Sanwal, D. et al. 2002, ApJ, 569, 894
Zhang, B., & Harding, A. K. 2000, ApJ, 532, 1150
Zhang, L., & Cheng, K. S. 1997, ApJ, 487, 370